Cell

State-Dependent Architecture of Thalamic Reticular Subnetworks

Michael M. Halassa,[1,2,3,4,*] Zhe Chen,[3] Ralf D. Wimmer,[1,2,3,4] Philip M. Brunetti,[4] Shengli Zhao,[5] Basilis Zikopoulos,[6] Fan Wang,[5] Emery N. Brown,[7,8,9,10] and Matthew A. Wilson[4]
[1]Neuroscience Institute, New York University Langone Medical Center, New York, NY 10016, USA
[2]Department of Neuroscience & Physiology, New York University Langone Medical Center, New York, NY 10016, USA
[3]Department of Psychiatry, New York University Langone Medical Center, New York, NY 10016, USA
[4]Picower Institute for Learning and Memory, Massachusetts Institute of Technology, Cambridge, MA 02139, USA
[5]Department of Cell Biology, Duke University, Durham, NC 27710, USA
[6]Department of Health Sciences and Program in Neuroscience, Boston University, Boston, MA 02215, USA
[7]Department of Anesthesia, Critical Care and Pain Medicine, Massachusetts General Hospital, Boston, MA 02114, USA
[8]Harvard Medical School, Boston, MA 02115, USA
[9]Department of Brain and Cognitive Sciences, Massachusetts Institute of Technology, Cambridge, MA 02139, USA
[10]Harvard-MIT Division of Health Sciences and Technology, Institute of Medical Engineering and Science, Massachusetts Institute of Technology, Cambridge, MA 02139, USA
*Correspondence: michael.halassa@nyumc.org
http://dx.doi.org/10.1016/j.cell.2014.06.025

SUMMARY

Behavioral state is known to influence interactions between thalamus and cortex, which are important for sensation, action, and cognition. The thalamic reticular nucleus (TRN) is hypothesized to regulate thalamo-cortical interactions, but the underlying functional architecture of this process and its state dependence are unknown. By combining the first TRN ensemble recording with psychophysics and connectivity-based optogenetic tagging, we found reticular circuits to be composed of distinct subnetworks. While activity of limbic-projecting TRN neurons positively correlates with arousal, sensory-projecting neurons participate in spindles and show elevated synchrony by slow waves during sleep. Sensory-projecting neurons are suppressed by attentional states, demonstrating that their gating of thalamo-cortical interactions is matched to behavioral state. Bidirectional manipulation of attentional performance was achieved through subnetwork-specific optogenetic stimulation. Together, our findings provide evidence for differential inhibition of thalamic nuclei across brain states, where the TRN separately controls external sensory and internal limbic processing facilitating normal cognitive function.

INTRODUCTION

How does the brain switch between processing of information originating from different sources to successfully guide behavior? How does it flexibly shift between processing external stimuli and internal constructs to optimize cognitive performance? Answers to these questions will not only enhance our understanding of the neural basis of cognition but will also refine our concepts of brain disorders in which cognitive dysfunction is central (Stefansson et al., 2014). In humans, the shift between external and internal goal-directed cognition is known to recruit distinct cortical networks (Buckner and Krienen, 2013). For example, the default mode network, which includes medial prefrontal cortex, is suppressed during tasks that demand external attention but activated when subjects perform internally guided behaviors (Spreng et al., 2010). In contrast, the dorsal attentional network, which includes dorsolateral prefrontal cortex, is activated during external attention (Fox et al., 2005). Electrophysiological recordings in nonhuman primates have shown that interactions among circuits of the dorsal attentional network are achieved through synchronous oscillatory dynamics (Miller and Buschman, 2013). Prefrontal regions lead parietal regions in top-down attention, whereas parietal regions lead prefrontal ones in bottom-up attention (Buschman and Miller, 2007). Although the circuit mechanisms underlying the establishment of these cortical oscillatory dynamic states are incompletely understood, recent experiments have shown that the thalamus may play a central role in cortico-cortical synchrony required for cognitive performance (Saalmann et al., 2012). These findings add to established knowledge on the role of thalamus in regulating cortical dynamics in sleep (Magnin et al., 2010; Steriade and Llinás, 1988) but raise important mechanistic questions on how it regulates cortical activity in an arousal state-dependent manner, a prerequisite to understanding its precise role in cognitive function. Also, because the thalamus is functionally segregated into different nuclei (Jones, 2002), it may allow for establishing a multitude of cortical states depending on the type and number of nuclei engaged during a particular behavior.

Broad shifts in arousal offer an opportunity to study circuit mechanisms of how the brain switches between processing external stimuli and internally generated activity. Several studies have delineated cortical mechanisms by which processing of

sensory information is broadly suppressed during sleep (Issa and Wang, 2011; Livingstone and Hubel, 1981) but is enhanced in active waking (Livingstone and Hubel, 1981) and attentional states (Briggs et al., 2013; Desimone and Duncan, 1995), whereas others have established mechanisms by which offline limbic processing of memories is enhanced during sleep and quiet wakefulness (Buzsáki, 2010; Ji and Wilson, 2007; Karlsson and Frank, 2009). Within this framework, thalamo-cortical network engagement in processing of different information types is expected to occur in an arousal state-dependent manner.

The thalamic reticular nucleus (TRN), a group of GABAergic neurons that provides inhibitory control over thalamic nuclei, is strategically positioned to selectively modulate thalamo-cortical interactions (Crick, 1984; Pinault, 2004). In fact, based on its anatomical connections, Francis Crick postulated that "if the thalamus is the gateway to the cortex, the reticular complex might be described as the guardian of the gateway" (Crick, 1984). The TRN has been implicated in sensory processing where its neurons exhibit complex visual receptive fields (Vaingankar et al., 2012) and respond to deviant (oddball) auditory stimuli (Yu et al., 2009). In behaving primates, visual TRN neurons are modulated by selective attention (McAlonan et al., 2008). The TRN has also been linked to internal processing during sleep, where its activity is associated with sleep rhythms and behavior (Cueni et al., 2008; Espinosa et al., 2008; Huguenard and McCormick, 2007). TRN neurons are known to exhibit rhythmicity in relation to spindle oscillations (Steriade et al., 1986), 9–15 Hz dynamics that are observed in the cortex during sleep, which correlate with sleep stability (Dang-Vu et al., 2010), and sleep-dependent memory consolidation (Diekelmann and Born, 2010; Eschenko et al., 2006). How the TRN operates to support these different state-dependent functions is unclear, in part, due to a gap in knowledge about how its microcircuits are functionally organized. Physiological attributes of thalamic nuclei are known to depend on their anatomical connections (Jones, 1981), but the TRN has traditionally been viewed as a monolithic structure, with no link between its connectivity and function. Although recent work in primates has shown distinct connectivity patterns for sensory and limbic TRN (Zikopoulos and Barbas, 2012), the impact of these anatomical substrates on thalamo-cortical function has remained unknown given the lack of physiological studies.

We directly addressed this gap in knowledge by recording from TRN ensembles in naturally behaving mice. Our recordings revealed a previously unknown functional diversity among TRN microcircuits. Specifically, two functional subpopulations of neurons were identified that exhibited opposite modulation by sleep and attentional states. Connectivity and genetic-based dissection of these microcircuits revealed an anatomical basis for this functional segregation. Specifically, sensory-projecting neurons exhibited activity patterns consistent with inhibition of sensory processing during sleep but its augmentation during attentional states, whereas limbic-connected neurons exhibited little activity during sleep, likely enhancing offline limbic processing. TRN-specific optogenetic manipulations revealed its causal role in attentional performance, an effect that was recapitulated by its selective sensory subnetwork manipulation. Together, our data show that the TRN consists of connectivity-based functional subnetworks that differentially participate in sensory and limbic processing in a state-dependent manner. This architecture may facilitate switching of cortical information processing between externally driven and internally generated computations, a basic determinant of cognitive function.

RESULTS

TRN Recordings in the Freely Behaving Preparation

To obtain stable recordings of TRN ensembles in mice during free behavior, we implanted arrays of adjustable extracellular recording electrodes targeting the dorsal pole of this brain structure (Figure 1A), which is known to be connected to both anterior limbic (Cornwall et al., 1990) and visual sensory thalamic nuclei (Kimura et al., 2012). Electrode position was confirmed by physiological signals obtained during adjustment (Figures 1A–1D), and postmortem histology (Figures 1E and 1F). TRN neurons were identified by their thin spike waveform compared to relay neurons as has been done in recent studies (Gardner et al., 2013; Halassa et al., 2011) (Figure 1G) and is normally performed for extracellular inhibitory neuronal identification in cortical (Cardin et al., 2009) and hippocampal recordings (Royer et al., 2012). Consistent with previous studies, many TRN neurons showed a bursting spike firing pattern most noticeable during slow wave sleep (SWS; 128 out of 195; Figures S1A and S1B available online), and about half of these neurons exhibited a particular burst structure (accelerando decelerando) observed in other species (Marlinski et al., 2012; Vaingankar et al., 2012) (Figures S1C and S1D).

TRN Neurons Exhibit Heterogeneous Firing in Relation to Sleep Spindle Oscillations

One of the major functions attributed to TRN neurons is their role in generating spindle oscillations (Bazhenov et al., 2000; Contreras et al., 1993; Halassa et al., 2011). We examined the correlation between individual TRN neuronal rate functions and cortical electroencephalographic (EEG) spindle power in natural SWS (Figures 2A, S2A and S2B). Consistent with previous findings in unanesthetized cats (Steriade et al., 1986), we found that many TRN neurons were positively correlated with spindle power (Figures 2A and S2B). However, surprisingly, we found that others were negatively correlated with this measure (Figures 2A and S2B). Analysis of the correlation between TRN neuronal firing rates and cortical spindle power revealed a bimodal distribution (Figure 2B; n = 7 mice). Neurons that were positively correlated to spindle power increased their firing rate specifically during spindle events (Figures 2C–2E; see Figures S2C and S2D for spindle detection examples), with stronger spindle-phase locking values observed for these neurons than negatively correlated ones (Figures 2F–2H; see Figures S2E and S2F for unbiased detection of phase locking). Conversely, neurons that were negatively correlated to spindle power were also negatively correlated to delta power (Figure S2G) and exhibited a robust elevation in firing rate with increased arousal (arousal correlated [AC]; Figure 2I). Thus, in SWS, two functional TRN subpopulations are observed: one that is spindle correlated (SC) and another that is AC. Equivalent numbers of these neurons were recorded from all animals with high recording yield, and they exhibited no difference in overall firing rates or burst properties (Table S1).

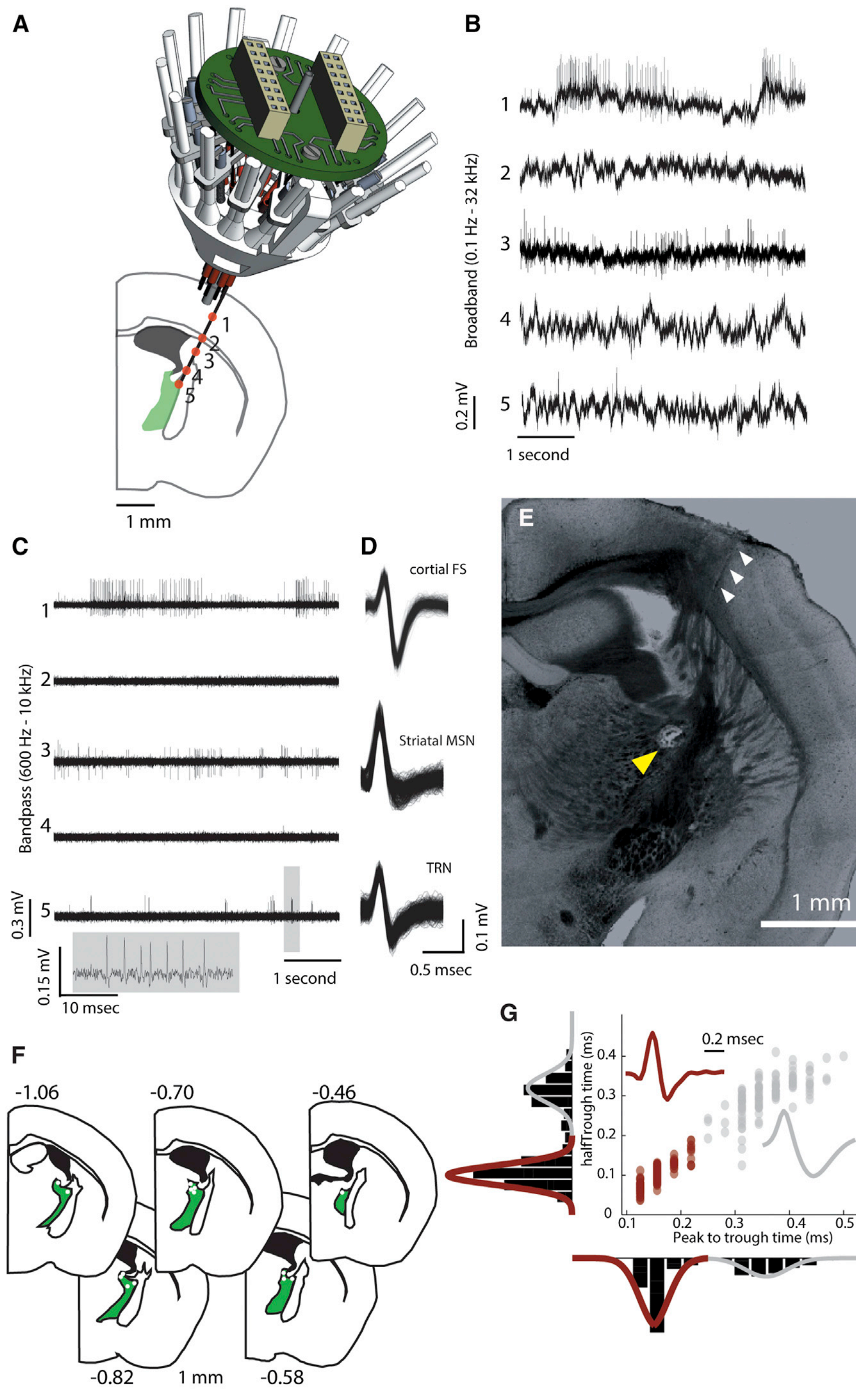

Figure 1. Independently Adjustable Multi-electrode Recordings in the TRN

(A) The dorsal part of TRN was targeted by implanting an independently adjustable multi-electrode implant (16 independently movable microdrives, only 6–12 loaded in any experiment) at a 15-degree angle relative to midline. Numbers denote different anatomical structures at which physiological recordings were made and shown in (B) and (C).

(B) Broadband (0.1 Hz–32 kHz) signal recorded at the different anatomical stations shows the physiological trajectory of the recordings. Note the absence of spiking in the two white matter crossings (corpus callosum [2] and internal capsule [4]).

(C) Band-pass filtered signal (600 Hz–10 kHz) of traces in (B) showing spike trains.

(D) Clustered neurons from traces 1, 3, and 5 showing the waveforms of a putative cortical fast-spiking interneuron (top), a striatal medium spiny neuron (middle), and finally, a TRN neuron (bottom). Highlighted inset shows a burst event of this unit, exhibiting the accelerando-decelerando burst structure previously described.

(E) Histological verification of the recording by electrode track (white arrowheads) and lesion at the tip (yellow arrowheads).

(F) Distribution of TRN lesions seen across six out of seven mice recorded. Numbers denote A/P distance from bregma in millimeters.

(G) A total of 195 putative TRN units with "thin" spikes were recorded (crimson), which had significantly different spike waveform features (peak-to-trough time and trough half-width) than 102 putative thalamic units (red).

See also Figure S1.

SC TRN Neurons Exhibit State-Dependent Modulation Consistent with Regulation of Sensory Processing

SWS is a state in which the cortical surface EEG is dominated by slow waves in the delta range (0.5–4 Hz). These dynamics are associated with coordinated changes of excitability across cortical neurons (Steriade et al., 1993; Vyazovskiy et al., 2009) and are known to influence excitability in cortically connected structures (Hahn et al., 2012). We found that TRN neurons were modulated by cortical delta, with both SC and AC neurons exhibiting comparable delta-phase locking values (Figures 3A–3D). However, whereas SC neurons showed preferred firing during delta wave troughs (corresponding to UP states, assessed by cortical multiunit activity), AC neurons showed a broad delta-phase distribution (Figures 3E and 3F). The narrow delta-phase distribution of SC neurons suggested an enhanced probability of coordinated spiking across this population, which was confirmed by a SWS-dependent increase in their spike time synchrony (a short-latency cross-correlation measure; see Experimental Procedures), compared to AC neurons (Figures 3G–3I and S3). Because sensory processing is known to be suppressed during sleep, this finding suggested that SC neuronal synchrony participates in this suppression by inhibiting thalamus. To explore whether this participation can extend to sensory processing during wake, we performed exploratory behavioral experiments requiring animals to detect a sensory stimulus (Kahn et al., 2012). We found that SC neurons were more likely to reduce their activity in the attentional phase of this visual detection task

compared to AC neurons (Figure S4). Together, these findings show selective participation of SC neurons in modulating sensory processing in both sleep and attentional states, suggesting that their arousal-dependent modulation determines their functional impact.

Optogenetics-Assisted Circuit Dissection of TRN Neurons Reveals Connectivity-Based Subnetwork Architecture

Because dorsal TRN projects to both sensory and limbic thalamus (Figure S5), we asked whether functional attributes of SC and AC neurons were related to patterns of connectivity with thalamic targets. To enable selective targeting of the TRN, we used mice that expressed Cre recombinase (Cre) under the vesicular γ-aminobutyric acid transporter (VGAT) promoter (Vong et al., 2011). VGAT-Cre animals enabled selective expression of transgenes in the TRN, but not nearby thalamic nuclei, which do not contain VGAT-positive neurons. This was achieved by injecting adeno-associated viruses (AAVs) containing double-floxed cassettes, stereotactically into the TRN (Figures S5A–S5F). To enable targeting of TRN neurons that project to specific thalamic nuclei, we used lentiviruses. These viruses exhibited two important attributes that resulted in connectivity-specific TRN neuronal tagging. First, because they were pseudotyped with a chimeric envelope protein composed of the extracellular and transmembrane domains of rabies virus glycoprotein (RG) and the cytoplasmic domain of vesicular stomatitis virus G protein (VSV-G) (see Experimental Procedures), they were taken up by axonal terminals in the thalamic target of interest and retrogradely transported. Second, these viruses were engineered to harbor double-floxed cassettes and, therefore, only resulted in the expression of transgenes in the TRN when injected in VGAT-Cre mice (Figures S5H–S5O). Using this strategy, we engineered retrograde lentiviruses (RG-LVs) with double-floxed cassettes containing the light-activated ion channel channelrhodopsin-2 (ChR2) (Boyden et al., 2005; Fenno et al., 2011) and injected them into either sensory visual or anterior limbic thalamus of VGAT-Cre mice (Figures 4A and 4B). We performed extracellular recordings from optogenetically identified TRN neurons in three visual- and two anterior-injected mice while animals performed a visual detection task and in posttask sleep (Figures 4C and 4E). We identified visual thalamic-projecting or anterior complex-projecting neurons by their short-latency response to 10 ms pulses of blue laser (5–10 ms onset; Figures 4D and 4F). Visual-projecting neurons also showed a 30–50 ms latency response to visual stimulation (Figures 4D and 4F). Electrode positions were additionally confirmed by postmortem histology (Figures 4G and 4H).

We found that visual-projecting TRN neurons were functionally different from limbic-projecting ones. Specifically, visual-connected neurons were mostly SC (Figure 5A), whereas limbic-projecting neurons were AC (Figures 5B and 5C). Visual-projecting neurons exhibited significantly higher phase locking to spindles than limbic-projecting neurons (Figure 5D). Consistent with a role for visual-projecting TRN in state-dependent control of visual processing, these neurons exhibited elevated pairwise spike time synchrony in SWS, whereas limbic-projecting neurons did not (Figure 5E).

To investigate the participation of these subnetworks in information processing beyond sleep, we trained mice on a visual detection task that required attentional engagement. The task required the animal to correctly detect a visual stimulus (500 ms) and subsequently move toward it, obtaining food from a reward site positioned underneath the stimulus location. A white noise auditory stimulus signaled the ability to initiate a trial. A trial was successfully initiated when the mouse broke an infrared beam continuously for 500–700 ms, ensuring proper head orientation during visual stimulus presentation. To minimize impulsive poking, rewards were only made available for a period of 15 s following successful initiation (Figure 5F). The absence of a correlation between initiation time and latency to collect reward as well as elevated latency during catch trials confirmed timely and specific response to visual stimulus presentation (Figures S6A–S6C). We found a robust and specific reduction in firing rate for visual-projecting TRN neurons following trial initiation, but no significant modulation of limbic-projecting TRN neurons during the task (Figure 5G). This result is consistent with the engagement of visual TRN subnetwork in state-dependent sensory visual processing. Furthermore, because the modulation occurred in the period prior to stimulus presentation, it suggested the participation of these neurons in attentional states, where visual thalamic inhibition may be transiently reduced to augment subsequent sensory processing.

Temporally Precise TRN Activation Diminishes Performance on the Visual Detection Task

To investigate whether the observed TRN neuronal firing rate changes were causal for visual detection task performance, we employed optogenetic manipulations. First, we injected a Cre-dependent AAV (serotype 2)-expressing channelrhodopsin into the TRN of VGAT-Cre mice, which resulted in selective TRN expression (Figure 6A). Because visual TRN neurons exhibited reduction in firing rate between task initiation and stimulus presentation, we used optogenetic activation to offset this reduction. Our investigations showed that pulse trains of >40 Hz (4–5 mW, 200 μm fiber [140–180 mW/mm]) result in sustained elevation of TRN neuronal firing rates and a concomitant reduction in their thalamic targets (Figure 6B). We therefore used pulse trains of 50 Hz frequency, pulse width 2 ms (duty cycle, 10%), to achieve a broad elevation of TRN firing rates throughout the initiation as well as stimulus presentation period (task stimulation). We found that this optogenetic stimulation regime resulted in a robust prolongation of latencies to collect reward in all mice examined (Figures 6C, 6E, S6D, and S6E; Movie S1). This suggested that enhancing TRN neuronal firing rate during the window of elevated attentional demands was detrimental to behavior, supporting the notion that a sharp drop in a subset of TRN neuronal firing rates was important for optimal performance. To test whether the optogenetic effect was a result of diminished stimulus perception, we delivered a laser stimulation train of similar length that started upon stimulus presentation but avoided the initiation period (Figure 6B). We found that this control stimulation did not impact performance on the task. Furthermore, in support of the specificity of the optogenetic effect to the initiation period, we found that pulse trains of only 500 ms limited to the postinitiation window resulted in diminished task

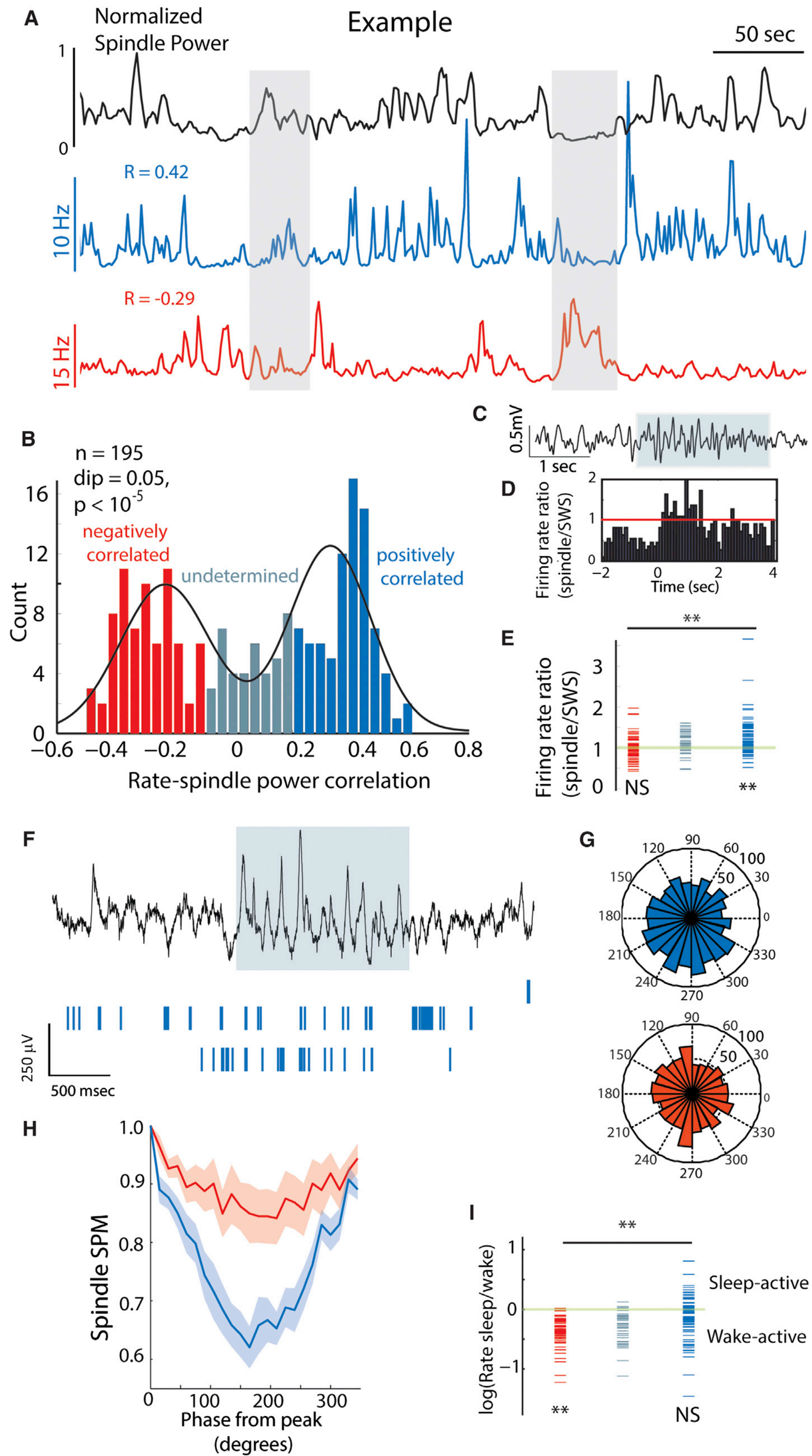

(legend on next page)

performance (Figures S6D and S6E). Also consistent with the notion that TRN stimulation did not interfere with stimulus perception, we found that this stimulation did not change the overall error rates in the task (Figures S6D and S6E).

Temporally Precise TRN Inhibition Enhances Attentional Performance

The negative impact of TRN stimulation on task performance was consistent with the requirement for a subset of its neurons to reduce their firing rate during the attentional window. To fully test the causality of these physiological observations in the context of the task, we used eNpHR3.0 (Deisseroth and Schnitzer, 2013; Tye et al., 2011), a light-activated Cl^- pump that is known to hyperpolarize neurons and inhibit spiking, to determine whether further reducing TRN firing rate would improve performance. To increase the likelihood of observing a behavioral modulation, we subjected mice to mild sleep deprivation (1–3 hr, at the beginning of their rest phase), which resulted in slightly diminished task performance evident by prolonged latencies ($p < 0.05$, rank sum test). Consistent with a causal role for TRN neurons in optimal task performance, we found that optogenetic inhibition of these neurons resulted in improved performance in all mice examined (Figures 6F–6H, S6F, and S6G; Movie S2).

To test whether these effects were subnetwork specific, we performed bidirectional optogenetic manipulations in retrogradely labeled TRN neuronal populations during the task (Figure 6I). We retrogradely labeled visual-connected and limbic-connected TRN neurons with either ChR2 or eNpHR3.0. We found that ChR2-mediated activation of the visual-projecting TRN during the attentional window of the visual detection task diminished performance, whereas its inhibition augmented performance. In contrast, neither activation nor inhibition of limbic-projecting TRN impacted performance (Figure 6J), consistent with the observation that these neurons are not significantly modulated during that phase of the task (Figure 5). These data also suggest that earlier results obtained with bidirectional manipulations of the TRN may be fully explained by effects on sensory-projecting neurons, a population that overlaps with the SC neurons identified earlier in this study. Our findings are unlikely to be explained by differences in optogenetic targeting because comparable proportions of TRN neurons were tagged in these two preparations (anterior projecting, 31 out of 100; visual projecting, 52 out of 190). In addition, there was no impact on error rates for any of these manipulations. Because the observed effects could be explained by neither sensory nor motor deficits, we suggest that they are likely cognitive. Also, because they occurred during the stimulus expectation period of the task, they are consistent with the involvement of TRN neurons in attentional states.

DISCUSSION

A major attribute of cognitive function is the ability to flexibly switch between processing different types of information. Broad shifts in arousal states offer an opportunity to examine how the brain switches from external stimulus processing during wake to internal memory processing during sleep. By regulating the interactions within thalamo-cortical networks, the TRN has been hypothesized to play an important role in cognitive function (Zikopoulos and Barbas, 2012). However, the precise nature of this regulation has been difficult to discern given the relative inaccessibility of TRN to physiological recordings. As such, and in the absence of concrete experimental data, the TRN has traditionally been viewed as a monolithic structure, providing uniform inhibition to thalamic nuclei (Crick, 1984; Llinás and Steriade, 2006). In such a regime, it is unclear how the brain would be able to selectively control the interactions between functionally segregated thalamic nuclei and their cortical targets.

In this study, we have systematically examined the functional architecture of the TRN in the freely behaving mouse. We found that the TRN is composed of functionally segregated subnetworks defined by anatomical connectivity. Sensory-projecting TRN regulates sensory processing in a state-dependent manner, whereas limbic-projecting TRN exhibits little activity during quiescent states, perhaps enabling the engagement of its thalamic target in offline processing associated with other limbic circuits (e.g., hippocampal reactivation). Additionally, inhibiting sensory-projecting TRN neurons during attentional states results in enhanced performance on a visual discrimination task, identifying this subnetwork as a possible target for cognitive enhancement (evident by reduced latency for sensory detection). Overall, our data show that the functional architecture of TRN subnetworks may have essential roles in mediating the impact of arousal states on higher-level cognitive function (Koch, 1993) and that it may be utilized in state-dependent switching between sensory transmission and offline processing (Figure 7).

Figure 2. Functional Segregation of TRN Subnetworks in SWS

(A) Two simultaneously recorded TRN neurons with time-varying firing rates that are positively and negatively correlated with cortical spindle power.

(B) Bimodal distribution (Hartigan's dip test, $p < 10^{-5}$) of this correlation across the data set (n = 195 TRN neurons, 7 mice). Gray represents the undetermined group (Experimental Procedures).

(C) Example of a detected EEG spindle.

(D) Peri-event time histogram (PETH) triggered by the onset of cortical spindles showing elevated firing rate of a positively correlated neuron (determined by analysis similar to A) during spindle events.

(E) This is significant across that population ($p < 10^{-8}$, rank sum test).

(F) Two positively correlated (to spindle power, as in A) TRN neuronal spike trains in relation to a spindle event.

(G) Spindle-phase histograms of two TRN neurons (red indicates negatively correlated; blue indicates positively correlated to spindle power, as in A). Note the higher phase locking for the positive-correlated neuron in this example.

(H) Tendency for higher spindle-phase locking in these neurons as a group (weighted mean ± SEM; rank sum test, p = 0.05 at the point of maximum modulation).

(I) Negatively correlated neurons are wake active ($p < 0.01$, rank sum test), whereas positively correlated neurons are state indifferent ($p < 0.0001$).

See also Figure S2 and Table S1.

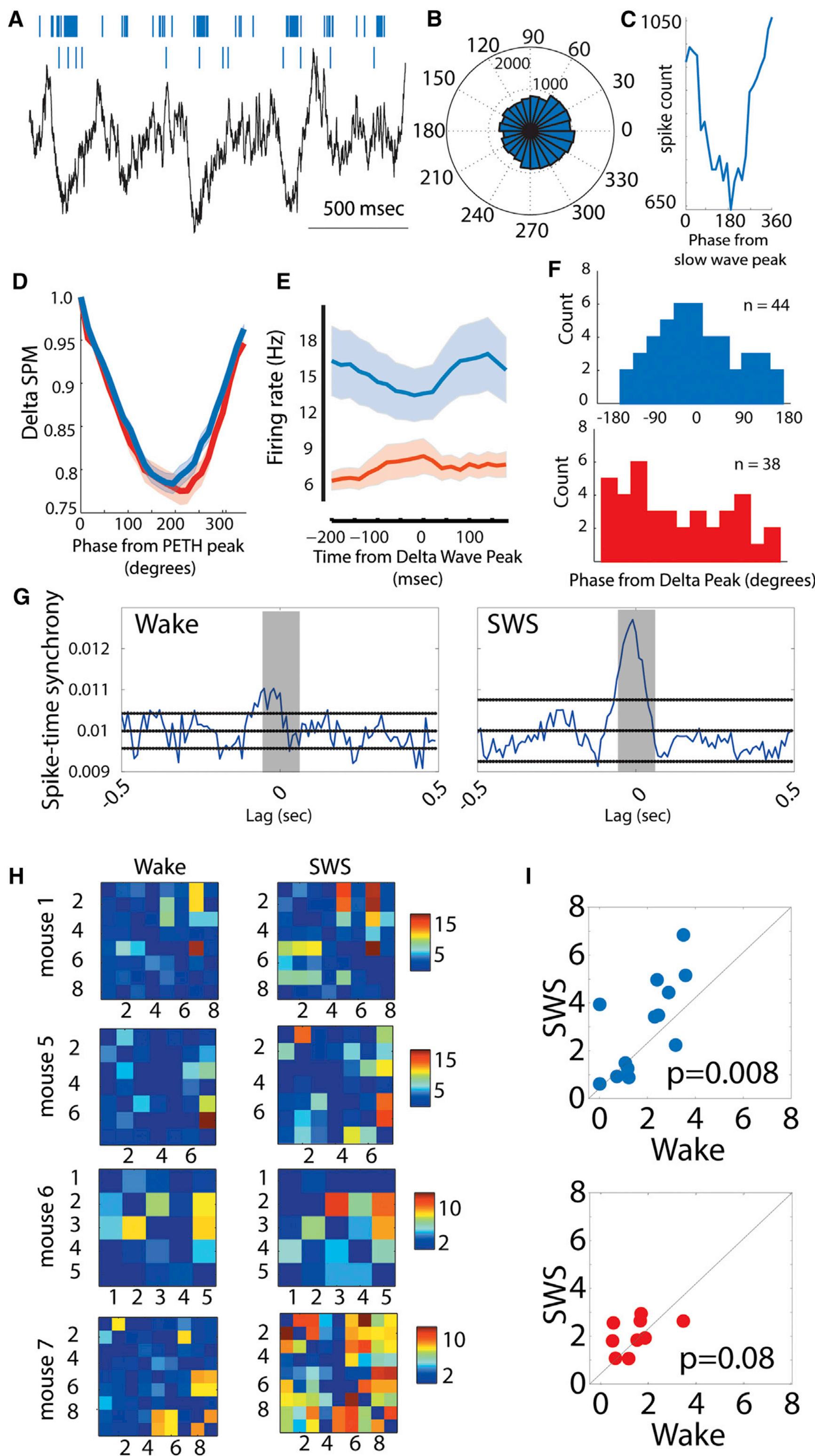

Figure 3. Enhanced Synchrony of SC Neurons during SWS

(A) During SWS, SC neuronal spiking occurs near cortical delta wave troughs.

(B and C) Spike delta-phase histogram of a SC neuron shows reduction of firing near the delta wave peaks.

(D) As a population, SC neurons exhibit comparable delta-phase locking to AC neurons (shaded area denotes the group SEM), shown in the depth of their spike-phase modulation (SPM).

(E) Delta wave peak-aligned PETH of the SC population (blue trace) shows stronger phase alignment to cortical delta oscillations than the AC population (red trace). Shaded area is SEM.

(F) Finding in (E) is further supported by plotting the histogram of the phase values (relative to delta wave peak) at which significantly modulated neurons exhibit minimum spike count. These distributions are significantly different (two-sample Kolmogorov-Smirnov test, $p < 0.03$). Note the peak in the SC neuron histogram, showing that these neurons exhibit little spiking around the peaks of delta oscillations.

(G) Example of spike time synchrony between two SC neurons (shaded area indicates −50 and 50 ms centered at zero lag) showing increased synchrony in SWS.

(H) Spike time synchrony (converted to *Z* score related to baseline) seen at the ensemble level (examples from four mice). Note the consistent overall elevation of spike time synchrony among SC units (mouse 1, n = 8; mouse 5, n = 7; mouse 6, n = 5; and mouse 7, n = 9) during SWS compared to wakefulness.

(I) Group analysis of these ensembles (SC: n = 13 ensembles from 4 mice, upper panel; AC: n = 9 ensembles from 4 mice, lower panel) shows an increase in SC subnetwork synchrony during SWS. Color bar indicates *Z* score. p values were obtained from signed-rank tests.

See also Figure S3.

Functionally Distinct TRN Subnetworks

Our initial recordings were in the dorso-rostral part of the mouse TRN (Figure 1), where reticular neurons are known to project to anterior (Cornwall et al., 1990) as well as visual sensory nuclei (Kimura et al., 2012) (Figure S5). In agreement with previous recordings in cats (Steriade et al., 1986), we found that many TRN neurons increased their firing rate with elevation in cortical spindle power. Our subsequent finding that visual sensory TRN neurons are likely to exhibit this attribute as well as phase lock to spindles is consistent with recordings from the somatosensory TRN in freely behaving rats (Marks and Roffwarg, 1993). The finding of a separate subpopulation of TRN neurons (AC) is unexpected, and its link to limbic processing might have been previously missed because earlier studies did not target limbic-projecting sectors of the TRN. In contrast to sensory-projecting TRN neurons, these neurons exhibited broad modulation by arousal state

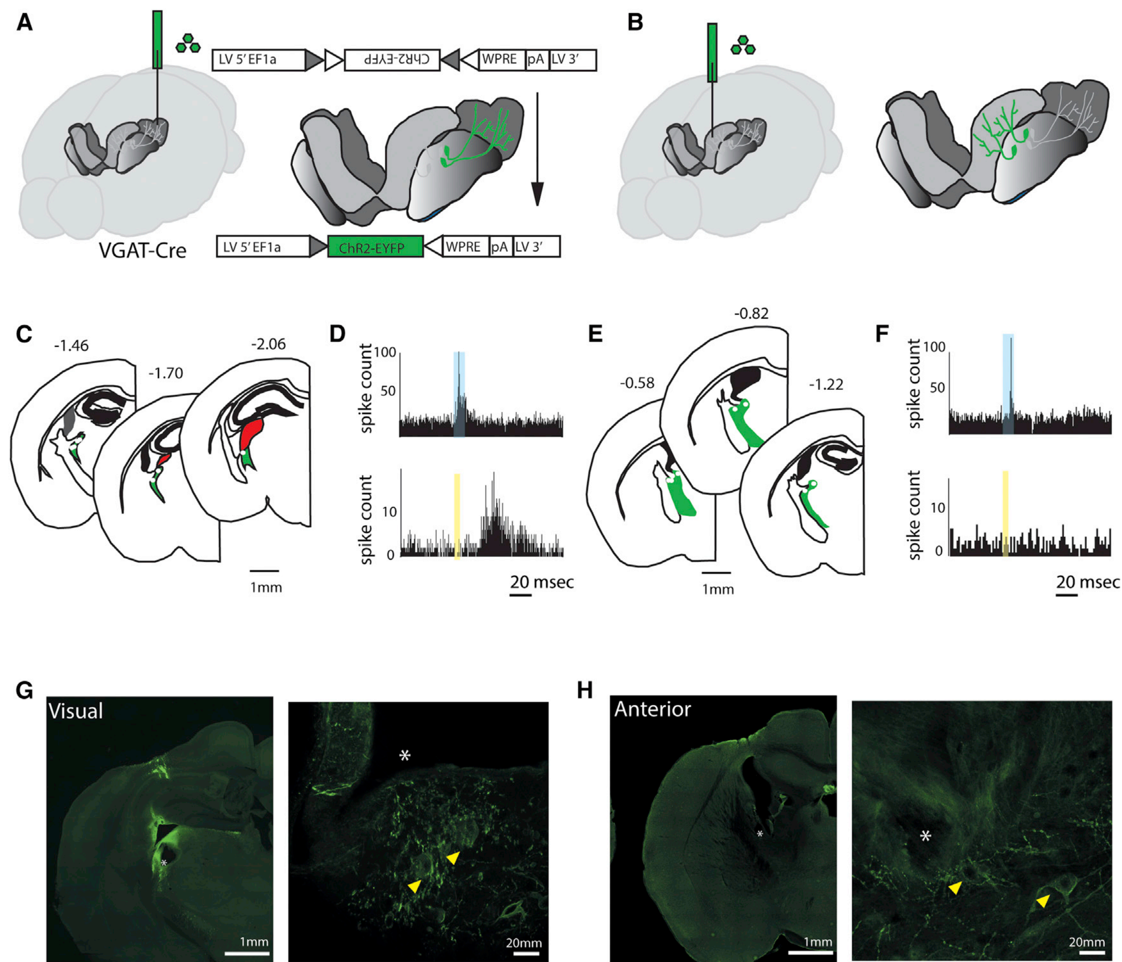

Figure 4. Optogenetic Tagging of TRN Neurons Based on Their Thalamic Targets

(A) Cartoon depiction of optogenetic tagging of visually connected TRN neurons in mice. A RG-LV containing a Cre-dependent ChR2-EYFP is injected into the visual thalamus of a VGAT-Cre mouse. Two to 4 weeks later, ChR2 is robustly expressed in visually connected TRN.

(B) Tagging of anterior complex-connected TRN, a similar procedure as in (A).

(C) Sections showing extracellular recording targets for visually connected TRN (n = 3 mice).

(D) Peri-stimulus time histograms (PSTHs) from two visual-tagged TRN neurons, showing optogenetic drive with short-latency responses (top) and visual drive with longer-latency responses (bottom).

(E and F) Similar depictions as in (C) and (D) but for anterior complex-projecting neurons.

(G) Example brain sections showing electrolytic lesions of electrode tips for visually connected TRN preparation. Confocal image on the right shows electrode tips (white asterisk) near neurons expressing ChR2-EYFP (yellow arrowheads).

(H) Similar figures to (G) but for anterior complex-tagged TRN neurons.

as seen in cortical (Vyazovskiy et al., 2009) and thalamocortical neurons (Weyand et al., 2001). Functional divergence of sensory and limbic TRN subnetworks was further evident during behavior in the visual detection task, where sensory neurons showed a sharp reduction in firing rate following task initiation (Figure 5), whereas limbic neurons did not. Interestingly, limbic-projecting neurons had comparable firing rates to AC neurons recorded in the first data set (Table S2 versus Table S1). However, visual-projecting neurons had different firing rates than SC neurons recorded earlier in the study. This may have been related to visual-projecting neurons being recorded from more caudal parts of the TRN (Figure 1 versus Figure 4).

The Impact of TRN on Cognitive Function

The reduction in firing rate observed for sensory TRN neurons during the task window in which attentional demands were highest suggests the engagement of these neurons in attentional state modulation. It is important to note that this modulation is probably distinct from the role of TRN in selective attention shown by studies in primates (McAlonan et al., 2008), which have revealed a correlation between neural responses and task accuracy, rather than speed. Our task has examined TRN involvement in the behavioral state preceding stimulus detection. Because mice perform this task with high accuracy, their variability in performance is seen mostly in latency, which is likely to reflect variability in attentional state (a form of arousal), rather

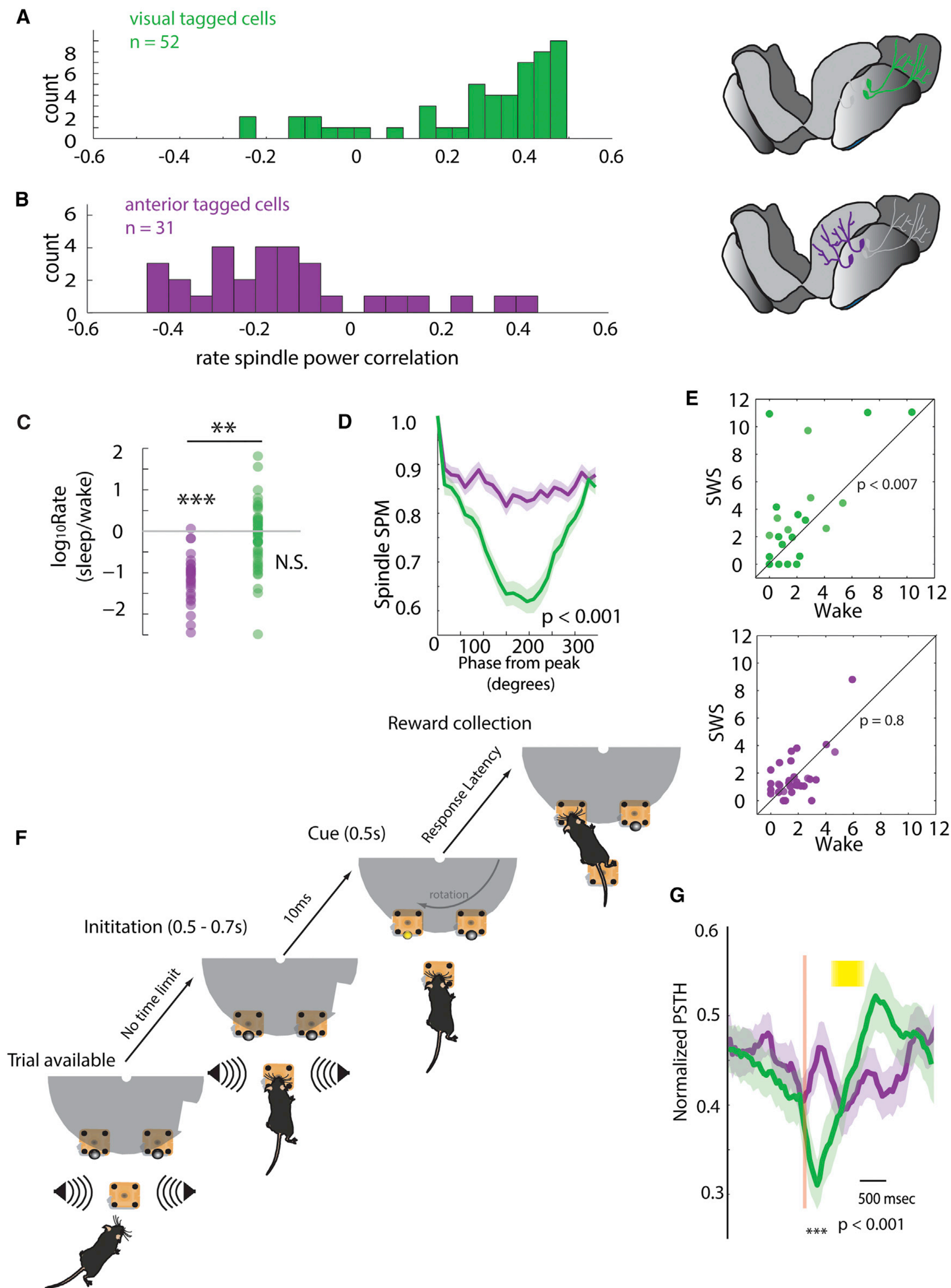

Figure 5. Intact TRN Microcircuit Dissection Connects Form to Function

(A and B) (A) Visual-tagged neurons are positively correlated to cortical spindle power in SWS ($p < 10^{-8}$, signed-rank test), but (B) anterior-tagged neurons are negatively correlated ($p = 0.006$).

(C) Anterior-tagged neurons are wake active, whereas visual-tagged neurons are state indifferent.

(D) Visual-tagged neurons show stronger phase locking to spindle oscillations ($p < 0.001$, rank sum test at the trough). Shaded area is SEM.

(legend continued on next page)

than selective attention. Our physiological results as well as optogenetic manipulations corroborate this notion, demonstrating that a reduction in sensory TRN firing rates is required for optimal task performance. Because neither a sensory nor motor effect was observed in these studies, we interpret these findings to reveal a permissive cognitive role for TRN in attentional states. This interpretation is consistent with the role of state-dependent cortical dynamics in accumulation of evidence required for decision making (Brunton et al., 2013; Kubanek et al., 2013).

The involvement of TRN in cognitive function offers a unique perspective on connecting a number of concepts in neuroscience that had previously been studied separately. For example, whereas our study examined the participation of TRN microcircuits in sleep and attentional states separately, the subnetwork architecture of TRN may allow for flexible switching between processing of external input and internal constructs in cognitive tasks, facilitating selective thalamo-cortical network engagement (Roth et al., 2009). Interestingly, recent experiments in humans have shown that rapid changes in arousal measures, such as pupil diameter, predict successful performance on cognitive tasks requiring the use of external information to update internal beliefs (Nassar et al., 2012). Given the state-dependent modulation of TRN neurons, these microcircuits may offer a mechanistic link between subtle changes in arousal and cognitive performance. In addition, these subnetworks offer a mammalian example of how the same neurons can switch their functionality in a behaviorally relevant manner, a long-recognized attribute of small circuits in model systems (Bargmann and Marder, 2013).

Our findings also offer a unique perspective on cognitive dysfunction, which appears to be central to a number of neurodevelopmental and neuropsychiatric disorders (Coe et al., 2012; Stefansson et al., 2014). Although inhibitory circuits have long-been recognized to be disrupted in several of these disorders, the focus has been on cortical interneurons (Gonzalez-Burgos and Lewis, 2012). Dissecting TRN microcircuit architecture and examining its participation in cognitive function are first steps in understanding how its dysfunction may contribute to brain disorders. Given the role of thalamus in regulating cortical states, it would not be surprising that its inhibitory dysfunction contributes to a number of brain disorders (Barch and Ceaser, 2012; Fitzgerald et al., 2000).

Spindle-Related Microcircuitry

Our findings that TRN neurons associated with spindle oscillations influence thalamic sensory processing in a state-dependent fashion provide a mechanism for the link between spindles and sleep stability (Dang-Vu et al., 2010; Wimmer et al., 2012). In addition, they link sensory processing in sleep to that during attentional states, which, to our knowledge, has never been explicitly demonstrated. Spindle-associated TRN microcircuits, controlling sensory processing across states of vigilance, may explain the long-recognized association between spindles and cognitive performance (Fogel and Smith, 2011) and may relate to the association between spindles and cognitive dysfunction in schizophrenia (Ferrarelli et al., 2010; Keshavan et al., 2011).

Relevance to Offline Processing

Could our findings be placed in a larger context of hippocampal-thalamo-cortical interaction underlying online behavior versus offline memory processing? We think yes. The hippocampus sends monosynaptic input to cingulate and retrosplenial cortices, areas that are connected to the anterior thalamic complex. Damage to any of these structures is known to result in spatial memory deficits (Rolls, 2013). As such, limbic TRN activity may be permissive to offline hippocampal-thalamo-cortical interactions evident by reduced firing rate of these neurons during SWS (Figure 5). The elevated firing of these neurons during active wakefulness may set a higher inhibitory tone in the anterior complex during behavioral arousal. The role of this inhibition in shaping online processing of these neurons, and their engagement in behavior, is an open but intriguing question.

The role of hippocampus and associated limbic circuitry in memory processing extends well beyond sleep because hippocampal-cortical interactions are required for basic cognitive tasks requiring online encoding and retrieval of memories (Preston and Eichenbaum, 2013). Recent findings of default mode network engagement in these tasks suggest large network functional organization (Ward et al., 2014), in which thalamic modulation of cortical dynamics may be necessary. The role of TRN in these large-scale functional interactions will undoubtedly be an exciting area of investigation, with broad basic and translational implications.

EXPERIMENTAL PROCEDURES

Animals

Seven 4- to 6-month-old male mice in a C57Bl6/J background were used for the first data set (Figures 1, 2, and 3). Three VGAT-Cre mice were used for visual thalamic optogenetic tagging, and two mice were used for anterior thalamic optogenetic tagging (Figures 4 and 5). Four VGAT-Cre mice were used for the optogenetic-activation experiments, and four others were used for the optogenetic inhibition (Figure 6). A total of seven VGAT-Cre mice were used for histology experiments (Figure S1). All research involving mice has been conducted according to the Institutional Animal Care and Use Committee (IACUC) guidelines at Massachusetts Institute of Technology. All procedures were approved by the IACUC.

Electrophysiological Recording

Following recovery, each animal was connected to two 16-channel preamplifier headstages or a single, custom-made 32-channel preamplifier headstage

(E) Visual-, but not anterior-, tagged neurons exhibit enhanced pairwise spike time synchrony in SWS (p values, signed-rank test; numbers of axes denote *Z* scores).

(F) Visual detection task design ensures control over psychophysical parameters. The mouse is informed of a new trial by a white noise stimulus emitted from two side speakers. To initiate a trial, the mouse is required to hold its snout in a nose poke for a period of 0.5–0.7 s, ensuring that when the 0.5 s stimulus is presented at one of the reward nose pokes, the head is in the correct orientation to see it. The rotating disk ensures that the reward sites are only available following the stimulus, minimizing impulsive poking behavior.

(G) Only visual-tagged neurons show a reduction in firing rate (group mean ± SEM; $p < 0.001$, rank sum test) during the attentional window of the visual detection task (yellow bar indicates stimulus).

See also Table S2.

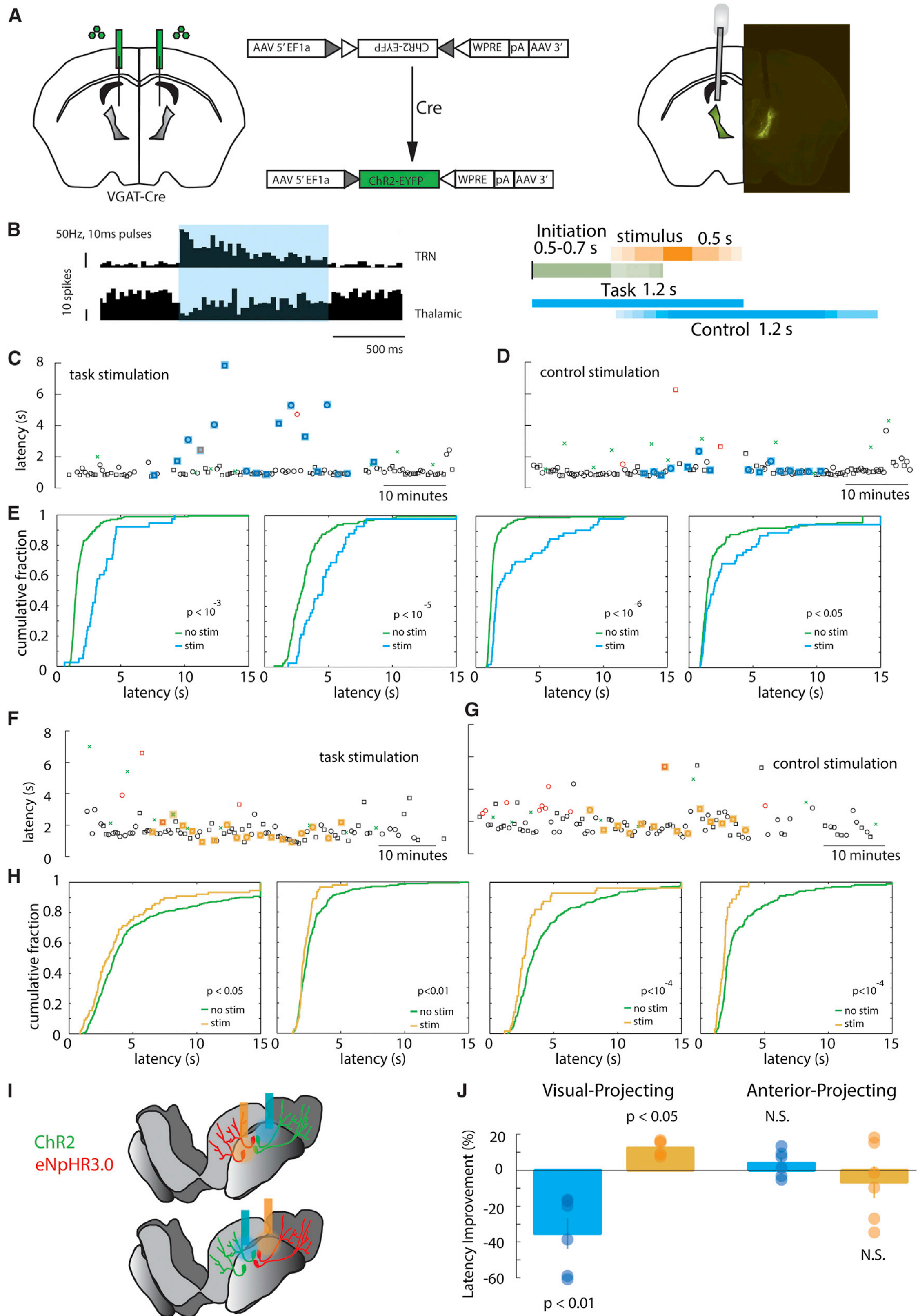

(legend on next page)

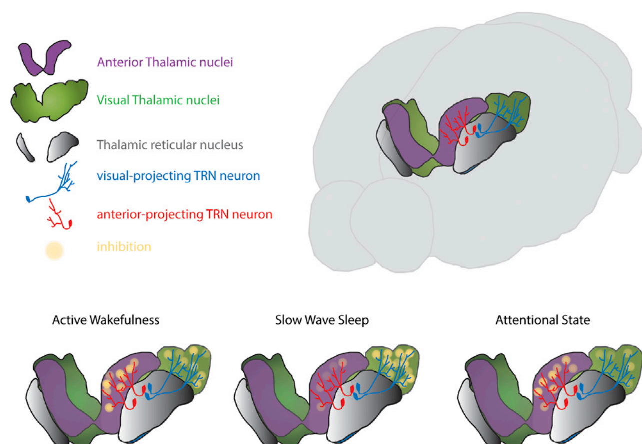

Figure 7. Cartoon Depiction of State-Dependent Thalamic Inhibition
During active wakefulness, inhibition in sensory and limbic thalamic nuclei is balanced. As the brain transitions to SWS, synchrony among sensory TRN neurons results in enhanced inhibition of sensory thalamic nuclei contributing to gating of external input. The reduction in firing rate of limbic-connected neurons is likely to result in reduced inhibition in limbic thalamus, perhaps facilitating offline processing. During attentional states, sensory neuronal firing rate is reduced, contributing to enhanced sensory thalamic engagement in processing of external stimuli. Although limbic thalamic neurons do not show an overall change in firing rate during these states, individual neurons may participate in shaping limbic processing during these states.

(Neuralynx). All data were recorded using a Neuralynx DigiLynx recording system. Signals from each stereotrode were amplified, filtered between 0.1 Hz and 9 kHz, and digitized at approximately 30 kHz. Local field potentials (LFPs) were collected from a single channel on each stereotrode. The LFP and EEG traces were amplified and filtered between 0.1 Hz and 30 kHz. The EEG was acquired as a referential signal between the ipsilateral frontal lead (at approximately anteroposterior [A/P], +0.5 mm; mediolateral [M/L], 0.5 mm; and dorsoventral [D/V], 0.1–0.2 mm, directed at cingulate) and cerebellar reference. For experiments involving the tagging of visual neurons, the EEG was a referential signal between primary visual cortex and the cerebellum. Stereotrodes were slowly lowered (over several days) in 125–250 μm steps. Spike sorting was performed offline using the MClust toolbox (http://redishlab.neuroscience.umn.edu/mclust/MClust.html), based on spike amplitudes and energies on the two electrodes of each stereotrode. Units were separated by hand, and cross-correlation and autocorrelation analyses were used to confirm unit separation.

Virus Injections

For anatomical-tracing experiments, AAV-hSyn-DIO-EGFP (serotype 2) was injected at multiple volumes (200 nl–1 μl) into thalamus of VGAT-Cre animals (A/P, −0.6 to −1.0 mm; M/L, 0.9 mm; and D/V, −3.5 mm) unilaterally. Animals were allowed to recover for at least 3 weeks for optimal virus expression, after which they were prepared for histological experiments.

For optogenetic manipulation experiments, AAV-EF1α-DIO-ChR2-EYFP and AAV-EF1α-DIO-eNpHR3.0-EYFP (all serotype 2) were used. These viruses were produced by the vector core at University of North Carolina, Chapel Hill, with titers around 10^{12} VG/ml. Viruses (250–350 nl) were injected bilaterally into TRN of VGAT-Cre mice (A/P, −0.6 mm; ±M/L, 0.9 mm; and D/V, −3.5 mm) using a quintessential stereotactic injector (Stoelting; #53311). Mice were allowed to recover for 2–4 weeks following injection to allow for virus expression. For retrograde histological tracing and optogenetic-tagging experiments (Figures 5 and S5), pseudotyped RG-LVs were used. Visually connected TRN neurons were labeled through virus injections (0.5–0.8 μl) into visual thalamus (AP, −2.1 mm; ML, 2 mm; and DV, 2.5 mm), whereas anterior thalamic-connected TRN neurons were targeted through injections into the anterior complex (AP, −0.7 mm; ML, 0.65 mm; and DV, −2.6 mm). RG-LV contained the EF1α promoter, followed by a double-flox cassette in which the floxed gene (in reverse orientation) was EGFP, channelrhodopsin (ChR2), or halorhodopsin (eNpHR3.0) and was followed by the woodchuck posttranscriptional regulatory element (WPRE). All vectors were modified from the original lentivector pFCGW. For production of the viral vector, the expression plasmid along with two helper plasmids, Δ8.9 and FuG-B2 (a chimeric envelope protein composed of the extracellular and transmembrane domains of RG and the cytoplasmic domain of VSV-G; pCAGGS-FuG-B2 [a gift from Kazuto Kobayashi, Fukushima Medical University, Fukushima]), were transfected into human embryonic kidney 293T cells with Lipofectamine 2000 (Invitrogen). Viral particles were collected from the cell culture medium, pelleted by ultracentrifugation at 65,000 × g (m/s^2) for 2.5 hr, resuspended in PBS, washed, and concentrated using Amicon Ultra 4. Titers were between 10^8 and 10^9 VG/ml. Mice were allowed 4–6 weeks of recovery following surgery to allow for retrograde virus expression.

Online Optogenetic Tagging of TRN Units

A fiber-optic patch cord (Doric Lenses) delivered light from a 473 nm laser (Opto Engine) to the fiber-optic connector on the animal's implant. Prior to

Figure 6. Bidirectional Manipulation of Cognitive Performance by Selective TRN Targeting
(A) Schematic showing strategy for rendering the TRN optically sensitive. The TRN of a VGAT-Cre mouse is bilaterally injected with an AAV containing a double-floxed optogenetic molecule cassette (in this example ChR2-EYFP), which is flipped into frame only in Cre-expressing neurons. Because thalamic relay nuclei are largely devoid of VGAT-expressing neurons (except for LGN, which is sufficiently far away from the injection site), ChR2-EYFP expression is limited to the TRN. A similar strategy is used for eNpHR3.0-EYFP experiments (F–H).
(B) Left: two PSTHs of a TRN unit and a thalamic unit in response to a 50 Hz laser stimulus (2 ms pulse duration, 1 s duration), showing broad elevation in spiking for the TRN unit and broad suppression of spiking in the thalamic unit. Right panel is a timeline of optogenetic stimulation regimes in relation to task phases. The same strategy is adopted for optogenetic inhibition.
(C and D) Examples of a selective TRN stimulation session carried out during all task phases (C) or avoiding the initiation phase, but of similar length, "control stimulation" (D). Note the increased number of long-latency trials in the task stimulation but not the control one: black circle indicates left correct trial, black square indicates right correct trial, red circle indicates left incorrect trial, red square indicates right incorrect trial, and green cross indicates catch trials; laser trials are highlighted in blue.
(E) Cumulative distribution of trial latencies (to collect reward) from individual mice, showing diminished performance following TRN activation during the task in all four mice.
(F and G) Example sessions for eNpHR3.0-mediated TRN inhibition as in (C) and (D).
(H) Cumulative distribution of trial latencies from individual mice in response to TRN inhibition in the task, showing the opposite behavioral effect to stimulation.
(I) Setup for subnetwork-specific optogenetic manipulations.
(J) Optogenetic activation and inhibition of TRN subnetwork projecting to visual thalamus diminish and enhance performance, respectively, whereas similar manipulations of the anterior-projecting TRN have an opposite but nonsignificant effect (n = 6 sessions, two mice for each manipulation; p values were obtained from signed-rank tests). Error bars are SEM.
See also Figure S6 and Movies S1 and S2.

connecting to the animal, laser power was measured and titrated to ~10 mW using a neutral density filter (Thorlabs). Power at the tip of the implanted fiber was ~50% of this value, based on measurements prior to surgery. Thus, there was 4–5 mW of power at the fiber tip or 140–180 mW/mm for a 200 μm fiber. An analog stimulus generator was used to control laser pulses of 10 ms duration and 0.01 Hz frequency. See Extended Experimental Procedures for more information.

SUPPLEMENTAL INFORMATION

Supplemental Information includes Extended Experimental Procedures, six figures, two tables, and two movies and can be found with this article online at http://dx.doi.org/10.1016/j.cell.2014.06.025.

AUTHOR CONTRIBUTIONS

M.M.H. conceived and designed all aspects of the study and collected data. M.M.H. and Z.C. analyzed the electrophysiological and behavioral data. Z.C. developed computational methods for data analysis. R.D.W. and P.M.B. developed the attentional task. R.D.W. collected data for the optogenetic tagging experiments. S.Z. and F.W. provided retrograde viruses. B.Z. developed and adapted quantitative structural connectivity methods and provided input on their inclusion in the manuscript. E.N.B. provided input and oversight on statistical analysis. M.A.W. supervised the study. M.M.H. wrote the paper with input from M.A.W.

ACKNOWLEDGMENTS

We thank L. Acsady and T. Fellin for helpful comments, as well as all members of the M.A.W. laboratory. M.M.H. is supported by an NIH pathway to independence career award (K99 NS 078115) from the NINDS and a NARSAD Young Investigator Award. Z.C. is supported by an NSF-CRCNS grant (award IIS-1307645) and an Early Career Award (Mathematical Biosciences Institute). B.Z. is supported by grants from NIMH (R01MH101209 and R01MH057414) and NSF (CELEST and SBE-0354378). F.W. is supported by NIH grants (R01NS077986 and DP1MH103908). E.N.B. and M.A.W. are supported by a transformative R01 award (TR01-GM10498). M.A.W. is additionally supported by NIH grant R01-MH061976.

Received: March 5, 2014
Revised: May 22, 2014
Accepted: June 6, 2014
Published: August 14, 2014

REFERENCES

Barch, D.M., and Ceaser, A. (2012). Cognition in schizophrenia: core psychological and neural mechanisms. Trends Cogn. Sci. *16*, 27–34.

Bargmann, C.I., and Marder, E. (2013). From the connectome to brain function. Nat. Methods *10*, 483–490.

Bazhenov, M., Timofeev, I., Steriade, M., and Sejnowski, T. (2000). Spiking-bursting activity in the thalamic reticular nucleus initiates sequences of spindle oscillations in thalamic networks. J. Neurophysiol. *84*, 1076–1087.

Boyden, E.S., Zhang, F., Bamberg, E., Nagel, G., and Deisseroth, K. (2005). Millisecond-timescale, genetically targeted optical control of neural activity. Nat. Neurosci. *8*, 1263–1268.

Briggs, F., Mangun, G.R., and Usrey, W.M. (2013). Attention enhances synaptic efficacy and the signal-to-noise ratio in neural circuits. Nature *499*, 476–480.

Brunton, B.W., Botvinick, M.M., and Brody, C.D. (2013). Rats and humans can optimally accumulate evidence for decision-making. Science *340*, 95–98.

Buckner, R.L., and Krienen, F.M. (2013). The evolution of distributed association networks in the human brain. Trends Cogn. Sci. *17*, 648–665.

Buschman, T.J., and Miller, E.K. (2007). Top-down versus bottom-up control of attention in the prefrontal and posterior parietal cortices. Science *315*, 1860–1862.

Buzsáki, G. (2010). Neural syntax: cell assemblies, synapsembles, and readers. Neuron *68*, 362–385.

Cardin, J.A., Carlén, M., Meletis, K., Knoblich, U., Zhang, F., Deisseroth, K., Tsai, L.H., and Moore, C.I. (2009). Driving fast-spiking cells induces gamma rhythm and controls sensory responses. Nature *459*, 663–667.

Coe, B.P., Girirajan, S., and Eichler, E.E. (2012). The genetic variability and commonality of neurodevelopmental disease. Am. J. Med. Genet. C. Semin. Med. Genet. *160C*, 118–129.

Contreras, D., Curró Dossi, R., and Steriade, M. (1993). Electrophysiological properties of cat reticular thalamic neurones in vivo. J. Physiol. *470*, 273–294.

Cornwall, J., Cooper, J.D., and Phillipson, O.T. (1990). Projections to the rostral reticular thalamic nucleus in the rat. Exp. Brain Res. *80*, 157–171.

Crick, F. (1984). Function of the thalamic reticular complex: the searchlight hypothesis. Proc. Natl. Acad. Sci. USA *81*, 4586–4590.

Cueni, L., Canepari, M., Luján, R., Emmenegger, Y., Watanabe, M., Bond, C.T., Franken, P., Adelman, J.P., and Lüthi, A. (2008). T-type Ca2+ channels, SK2 channels and SERCAs gate sleep-related oscillations in thalamic dendrites. Nat. Neurosci. *11*, 683–692.

Dang-Vu, T.T., McKinney, S.M., Buxton, O.M., Solet, J.M., and Ellenbogen, J.M. (2010). Spontaneous brain rhythms predict sleep stability in the face of noise. Curr. Biol. *20*, R626–R627.

Deisseroth, K., and Schnitzer, M.J. (2013). Engineering approaches to illuminating brain structure and dynamics. Neuron *80*, 568–577.

Desimone, R., and Duncan, J. (1995). Neural mechanisms of selective visual attention. Annu. Rev. Neurosci. *18*, 193–222.

Diekelmann, S., and Born, J. (2010). The memory function of sleep. Nat. Rev. Neurosci. *11*, 114–126.

Eschenko, O., Mölle, M., Born, J., and Sara, S.J. (2006). Elevated sleep spindle density after learning or after retrieval in rats. J. Neurosci. *26*, 12914–12920.

Espinosa, F., Torres-Vega, M.A., Marks, G.A., and Joho, R.H. (2008). Ablation of Kv3.1 and Kv3.3 potassium channels disrupts thalamocortical oscillations in vitro and in vivo. J. Neurosci. *28*, 5570–5581.

Fenno, L., Yizhar, O., and Deisseroth, K. (2011). The development and application of optogenetics. Annu. Rev. Neurosci. *34*, 389–412.

Ferrarelli, F., Peterson, M.J., Sarasso, S., Riedner, B.A., Murphy, M.J., Benca, R.M., Bria, P., Kalin, N.H., and Tononi, G. (2010). Thalamic dysfunction in schizophrenia suggested by whole-night deficits in slow and fast spindles. Am. J. Psychiatry *167*, 1339–1348.

Fitzgerald, K.D., Moore, G.J., Paulson, L.A., Stewart, C.M., and Rosenberg, D.R. (2000). Proton spectroscopic imaging of the thalamus in treatment-naive pediatric obsessive-compulsive disorder. Biol. Psychiatry *47*, 174–182.

Fogel, S.M., and Smith, C.T. (2011). The function of the sleep spindle: a physiological index of intelligence and a mechanism for sleep-dependent memory consolidation. Neurosci. Biobehav. Rev. *35*, 1154–1165.

Fox, M.D., Snyder, A.Z., Vincent, J.L., Corbetta, M., Van Essen, D.C., and Raichle, M.E. (2005). The human brain is intrinsically organized into dynamic, anticorrelated functional networks. Proc. Natl. Acad. Sci. USA *102*, 9673–9678.

Gardner, R.J., Hughes, S.W., and Jones, M.W. (2013). Differential spike timing and phase dynamics of reticular thalamic and prefrontal cortical neuronal populations during sleep spindles. J. Neurosci. *33*, 18469–18480.

Gonzalez-Burgos, G., and Lewis, D.A. (2012). NMDA receptor hypofunction, parvalbumin-positive neurons, and cortical gamma oscillations in schizophrenia. Schizophr. Bull. *38*, 950–957.

Hahn, T.T., McFarland, J.M., Berberich, S., Sakmann, B., and Mehta, M.R. (2012). Spontaneous persistent activity in entorhinal cortex modulates cortico-hippocampal interaction in vivo. Nat. Neurosci. *15*, 1531–1538.

Halassa, M.M., Siegle, J.H., Ritt, J.T., Ting, J.T., Feng, G., and Moore, C.I. (2011). Selective optical drive of thalamic reticular nucleus generates thalamic bursts and cortical spindles. Nat. Neurosci. *14*, 1118–1120.

Huguenard, J.R., and McCormick, D.A. (2007). Thalamic synchrony and dynamic regulation of global forebrain oscillations. Trends Neurosci. *30*, 350–356.

Issa, E.B., and Wang, X. (2011). Altered neural responses to sounds in primate primary auditory cortex during slow-wave sleep. J. Neurosci. *31*, 2965–2973.

Ji, D., and Wilson, M.A. (2007). Coordinated memory replay in the visual cortex and hippocampus during sleep. Nat. Neurosci. *10*, 100–107.

Jones, E.G. (1981). Functional subdivision and synaptic organization of the mammalian thalamus. Int. Rev. Physiol. *25*, 173–245.

Jones, E.G. (2002). Thalamic organization and function after Cajal. Prog. Brain Res. *136*, 333–357.

Kahn, J.B., Ward, R.D., Kahn, L.W., Rudy, N.M., Kandel, E.R., Balsam, P.D., and Simpson, E.H. (2012). Medial prefrontal lesions in mice impair sustained attention but spare maintenance of information in working memory. Learn. Mem. *19*, 513–517.

Karlsson, M.P., and Frank, L.M. (2009). Awake replay of remote experiences in the hippocampus. Nat. Neurosci. *12*, 913–918.

Keshavan, M.S., Montrose, D.M., Miewald, J.M., and Jindal, R.D. (2011). Sleep correlates of cognition in early course psychotic disorders. Schizophr. Res. *131*, 231–234.

Kimura, A., Yokoi, I., Imbe, H., Donishi, T., and Kaneoke, Y. (2012). Distinctions in burst spiking between thalamic reticular nucleus cells projecting to the dorsal lateral geniculate and lateral posterior nuclei in the anesthetized rat. Neuroscience *226*, 208–226.

Koch, C. (1993). Computational approaches to cognition: the bottom-up view. Curr. Opin. Neurobiol. *3*, 203–208.

Kubanek, J., Snyder, L.H., Brunton, B.W., Brody, C.D., and Schalk, G. (2013). A low-frequency oscillatory neural signal in humans encodes a developing decision variable. Neuroimage *83*, 795–808.

Livingstone, M.S., and Hubel, D.H. (1981). Effects of sleep and arousal on the processing of visual information in the cat. Nature *291*, 554–561.

Llinás, R.R., and Steriade, M. (2006). Bursting of thalamic neurons and states of vigilance. J. Neurophysiol. *95*, 3297–3308.

Magnin, M., Rey, M., Bastuji, H., Guillemant, P., Mauguière, F., and Garcia-Larrea, L. (2010). Thalamic deactivation at sleep onset precedes that of the cerebral cortex in humans. Proc. Natl. Acad. Sci. USA *107*, 3829–3833.

Marks, G.A., and Roffwarg, H.P. (1993). Spontaneous activity in the thalamic reticular nucleus during the sleep/wake cycle of the freely-moving rat. Brain Res. *623*, 241–248.

Marlinski, V., Sirota, M.G., and Beloozerova, I.N. (2012). Differential gating of thalamocortical signals by reticular nucleus of thalamus during locomotion. J. Neurosci. *32*, 15823–15836.

McAlonan, K., Cavanaugh, J., and Wurtz, R.H. (2008). Guarding the gateway to cortex with attention in visual thalamus. Nature *456*, 391–394.

Miller, E.K., and Buschman, T.J. (2013). Cortical circuits for the control of attention. Curr. Opin. Neurobiol. *23*, 216–222.

Nassar, M.R., Rumsey, K.M., Wilson, R.C., Parikh, K., Heasly, B., and Gold, J.I. (2012). Rational regulation of learning dynamics by pupil-linked arousal systems. Nat. Neurosci. *15*, 1040–1046.

Pinault, D. (2004). The thalamic reticular nucleus: structure, function and concept. Brain Res. Brain Res. Rev. *46*, 1–31.

Preston, A.R., and Eichenbaum, H. (2013). Interplay of hippocampus and prefrontal cortex in memory. Curr. Biol. *23*, R764–R773.

Rolls, E.T. (2013). Limbic systems for emotion and for memory, but no single limbic system. Cortex. Published online December 24, 2013. http://dx.doi.org/10.1016/j.cortex.2013.12.005.

Roth, J.K., Johnson, M.K., Raye, C.L., and Constable, R.T. (2009). Similar and dissociable mechanisms for attention to internal versus external information. Neuroimage *48*, 601–608.

Royer, S., Zemelman, B.V., Losonczy, A., Kim, J., Chance, F., Magee, J.C., and Buzsáki, G. (2012). Control of timing, rate and bursts of hippocampal place cells by dendritic and somatic inhibition. Nat. Neurosci. *15*, 769–775.

Saalmann, Y.B., Pinsk, M.A., Wang, L., Li, X., and Kastner, S. (2012). The pulvinar regulates information transmission between cortical areas based on attention demands. Science *337*, 753–756.

Spreng, R.N., Stevens, W.D., Chamberlain, J.P., Gilmore, A.W., and Schacter, D.L. (2010). Default network activity, coupled with the frontoparietal control network, supports goal-directed cognition. Neuroimage *53*, 303–317.

Stefansson, H., Meyer-Lindenberg, A., Steinberg, S., Magnusdottir, B., Morgen, K., Arnarsdottir, S., Bjornsdottir, G., Walters, G.B., Jonsdottir, G.A., Doyle, O.M., et al. (2014). CNVs conferring risk of autism or schizophrenia affect cognition in controls. Nature *505*, 361–366.

Steriade, M., and Llinás, R.R. (1988). The functional states of the thalamus and the associated neuronal interplay. Physiol. Rev. *68*, 649–742.

Steriade, M., Domich, L., and Oakson, G. (1986). Reticularis thalami neurons revisited: activity changes during shifts in states of vigilance. J. Neurosci. *6*, 68–81.

Steriade, M., Nuñez, A., and Amzica, F. (1993). A novel slow (< 1 Hz) oscillation of neocortical neurons in vivo: depolarizing and hyperpolarizing components. J. Neurosci. *13*, 3252–3265.

Tye, K.M., Prakash, R., Kim, S.Y., Fenno, L.E., Grosenick, L., Zarabi, H., Thompson, K.R., Gradinaru, V., Ramakrishnan, C., and Deisseroth, K. (2011). Amygdala circuitry mediating reversible and bidirectional control of anxiety. Nature *471*, 358–362.

Vaingankar, V., Sanchez Soto, C., Wang, X., Sommer, F.T., and Hirsch, J.A. (2012). Neurons in the thalamic reticular nucleus are selective for diverse and complex visual features. Front. Integr. Neurosci. *6*, 118.

Vong, L., Ye, C., Yang, Z., Choi, B., Chua, S., Jr., and Lowell, B.B. (2011). Leptin action on GABAergic neurons prevents obesity and reduces inhibitory tone to POMC neurons. Neuron *71*, 142–154.

Vyazovskiy, V.V., Olcese, U., Lazimy, Y.M., Faraguna, U., Esser, S.K., Williams, J.C., Cirelli, C., and Tononi, G. (2009). Cortical firing and sleep homeostasis. Neuron *63*, 865–878.

Ward, A.M., Schultz, A.P., Huijbers, W., Van Dijk, K.R., Hedden, T., and Sperling, R.A. (2014). The parahippocampal gyrus links the default-mode cortical network with the medial temporal lobe memory system. Hum. Brain Mapp. *35*, 1061–1073.

Weyand, T.G., Boudreaux, M., and Guido, W. (2001). Burst and tonic response modes in thalamic neurons during sleep and wakefulness. J. Neurophysiol. *85*, 1107–1118.

Wimmer, R.D., Astori, S., Bond, C.T., Rovó, Z., Chatton, J.Y., Adelman, J.P., Franken, P., and Lüthi, A. (2012). Sustaining sleep spindles through enhanced SK2-channel activity consolidates sleep and elevates arousal threshold. J. Neurosci. *32*, 13917–13928.

Yu, X.J., Xu, X.X., He, S., and He, J. (2009). Change detection by thalamic reticular neurons. Nat. Neurosci. *12*, 1165–1170.

Zikopoulos, B., and Barbas, H. (2012). Pathways for emotions and attention converge on the thalamic reticular nucleus in primates. J. Neurosci. *32*, 5338–5350.